

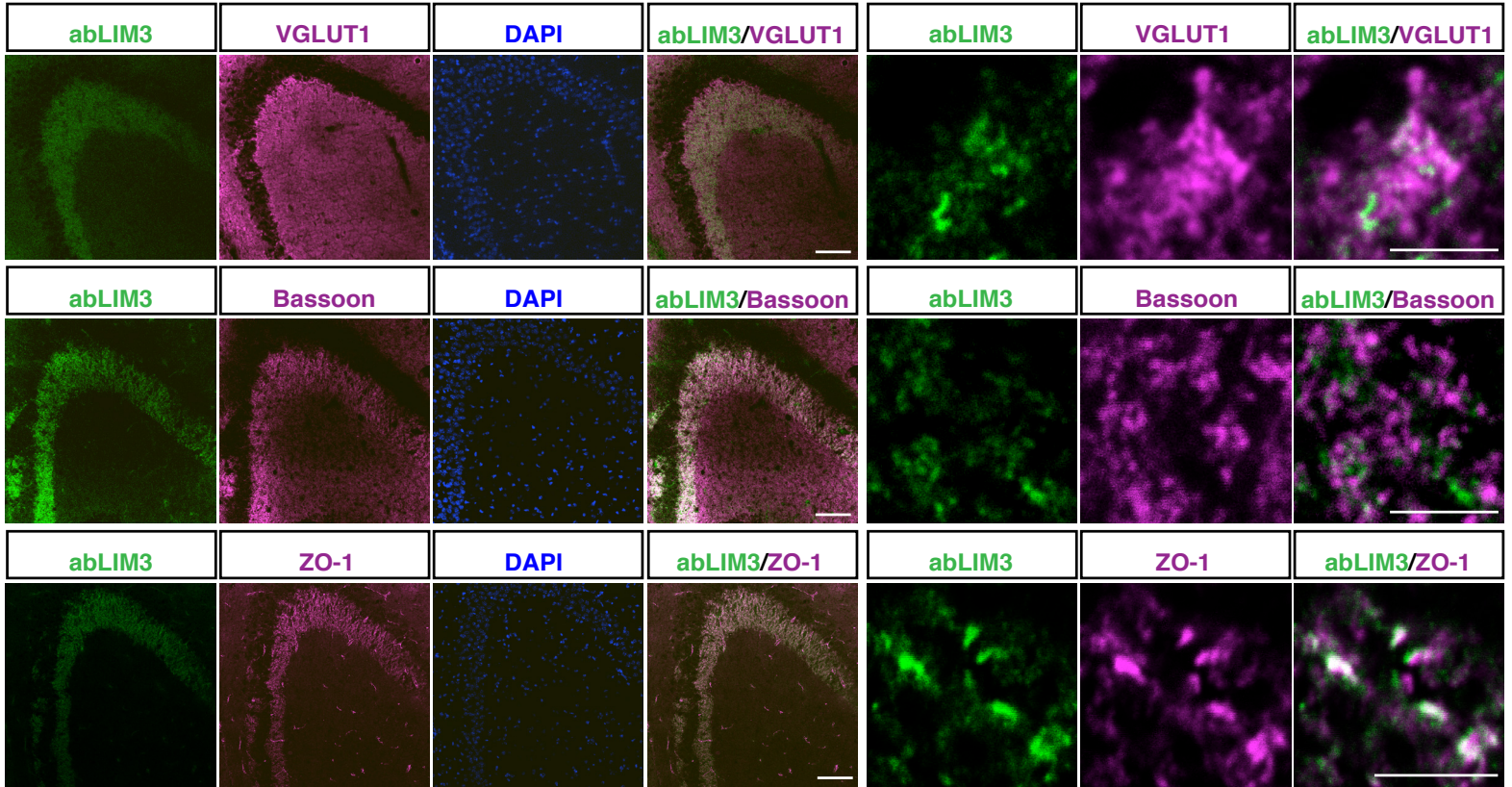
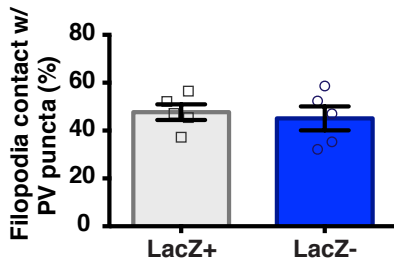
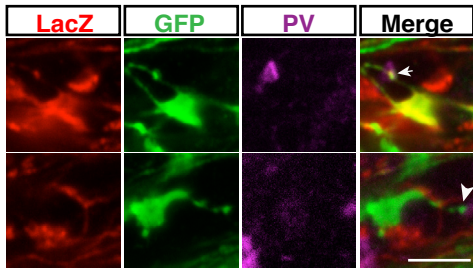
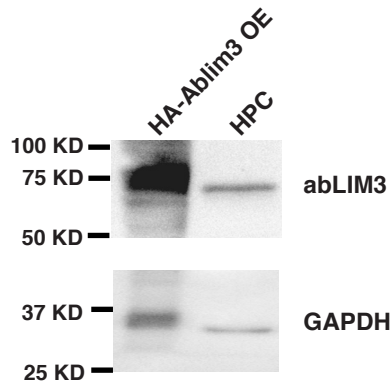
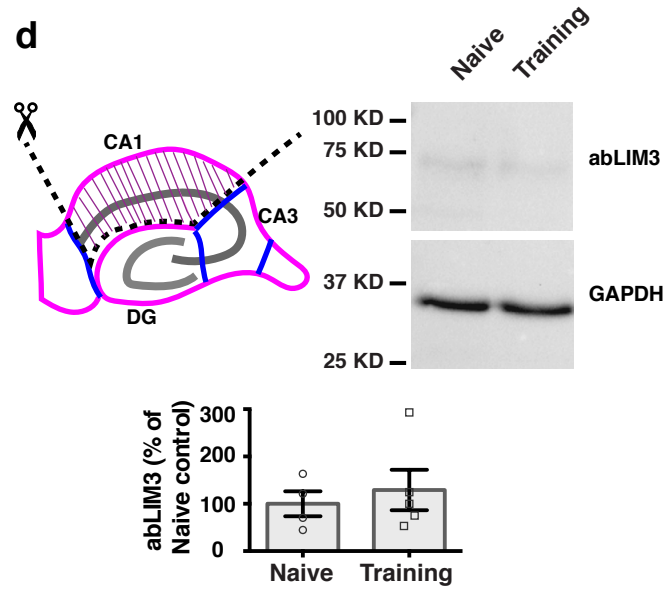
**Supplementary Figure 1. Temporal and spatial distribution of Actin Binding LIM Protein Family Member 3 (abLIM3) protein in DG.**

(a) Confocal triple immunofluorescence staining shows abLIM3 co-localization with ZO-1 (*lower*), but not Bassoon (*middle*), in VGLUT1 (*upper*) + MFTs in stratum lucidum of hippocampal CA3 region. Scale bar represents 100  $\mu$  m (*left 4 panels*) and 5  $\mu$  m (*right 3 panels*). This experiment was replicated 3 times.

(b) Images showing an ensemble+ MFT (LacZ+, *upper*) and ensemble- MFT (LacZ-, *lower*), and LacZ+ (arrow) and LacZ- (arrowhead) filopodial contacts with PV SLINs+. Bar graph showing quantification of MFT filopodial contacts with PV SLINs (150 filopodia extensions from LacZ+ MFTs and 232 filopodia extensions from LacZ- MFTs, n=5, 5 mice). Scale bar represents 5  $\mu$  m.

(c) Cell lysate from Transfected HEK293T cells following HA-abLIM3 overexpression (OE) was used as a positive control to validate abLIM3 antibody blotting of hippocampal (HPC) lysate. GAPDH served as loading control. This experiment was replicated twice. The representative image was cropped from full blot image shown in supplementary Fig. 11b.

(d) Schematic of dissection of CA1 subregion from hippocampus after contextual fear conditioning (*upper, left*). GAPDH as used as loading control. Western blot analysis showing abLIM3 levels are unchanged in the CA1 area of hippocampus following learning compared to naïve mice. Mice in training group were subjected to contextual fear conditioning and hippocampus was collected 1 h later (unpaired t-tests, n=4,5 mice). The representative image (*upper, right*) was cropped from full blot image shown in supplementary Fig. 11e. Bar graph (*lower*) showing protein levels was quantified from full blot image shown in supplementary Fig. 11e.

**a****b****c****d**

## Supplementary Figure 2. Validation of shRNAs to downregulate abLIM3 in DGCs

(a) Western blot analysis was performed to measure shRNA mediated knockdown of abLIM3 in 293K cells. Co-transfected GFP construct and endogenous Beta-actin were used as transfection and loading controls, respectively. The blot image was cropped from full blot image shown in supplementary Fig. 11a. This experiment was replicated 3 times.

(b) Schematic of lentiviral construct used for shNT/shRNA transduction (*upper*). Quantification of MFT size (*middle*) and filopodia length (*lower*) (n=3,3 mice) following lenti-shNT/shRNA#46/shRNA#47 injection into DG of 3-month old mice.

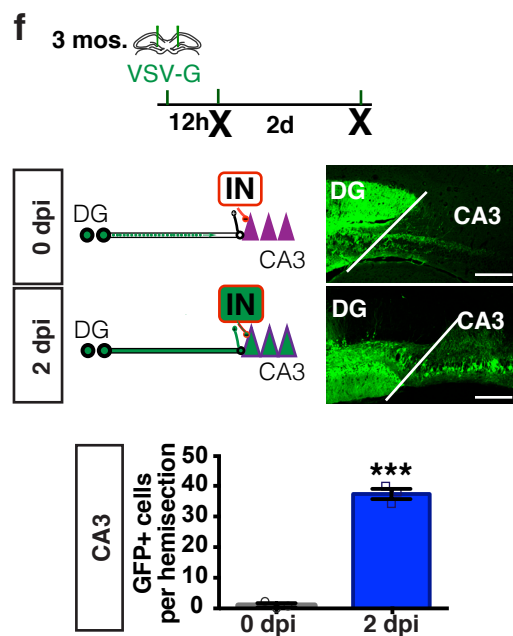
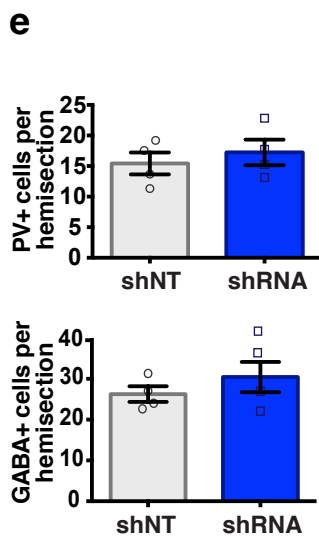
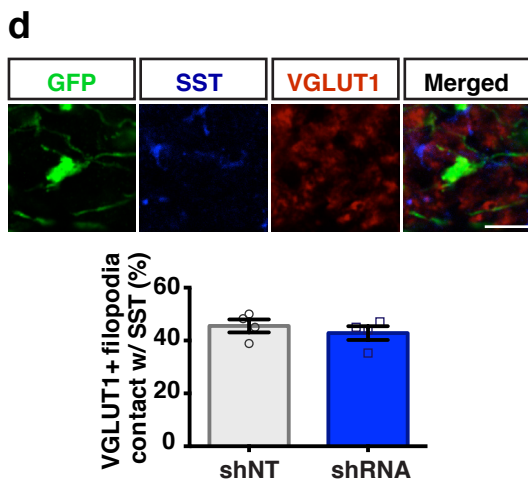
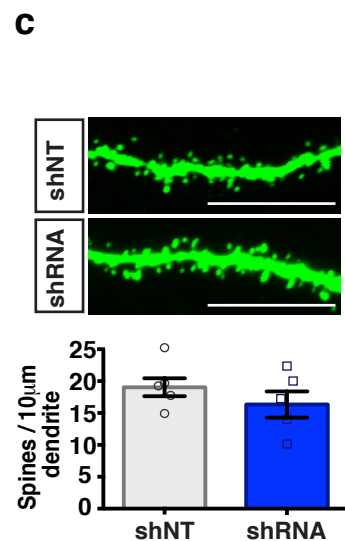
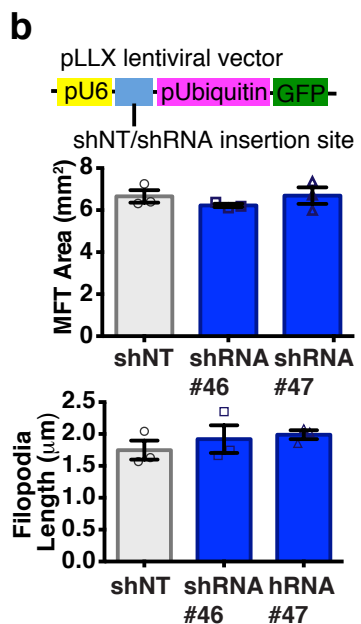
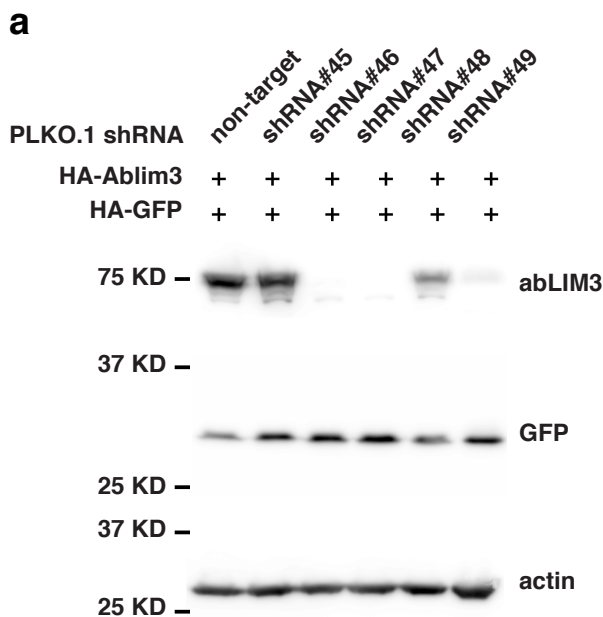
(c) Representative images show GFP+ dendrites in outer molecular layer (OML) following stereotaxic lentiviral-shNT/shRNA injection into DG (*upper*). Bar graph conveys quantification of DGC dendritic spines density (*lower*, n=5 mice for each group). Scale bar represents 10  $\mu$  m.

(d) Images showing VGLUT1+ MFT and MFT filopodia contacting SST SLINs (*upper*) and bar graphs with quantification of percentage of VGLUT1+ filopodia contacting SST (*lower*) (85 filopodial extensions in shNT group, 79 filopodial extensions in shRNA group, n=4,4 mice). Scale bar represents 5  $\mu$  m.

(e) Quantification showing total number of PV+ and GABA+ cells in CA3 of 3 months old mice (corresponds to Fig. 1i, n=4,4 mice).

(f) Schematic showing VSV-G injection into DG and schedule of analysis of mice at different time points following injection (*upper*). Schematic and representative images show anterograde labeled GFP+ cells in CA3 at day 2 but not 12 h post injection (*middle*). Bar graph conveying quantification of GFP+ cells in CA3 (*lower*, unpaired t-tests,  $P < 0.0001$ , n=3 mice for each group). Scale bar represents 50  $\mu$  m.

\*\*\* $p < 0.001$ , \*\* $p < 0.01$ , \* $p < 0.05$ . Data are represented mean  $\pm$  SEM.



**Supplementary Figure 3. Characterization of lentiviral-shRNA mediated knockdown of *Ablim3* in DG.**

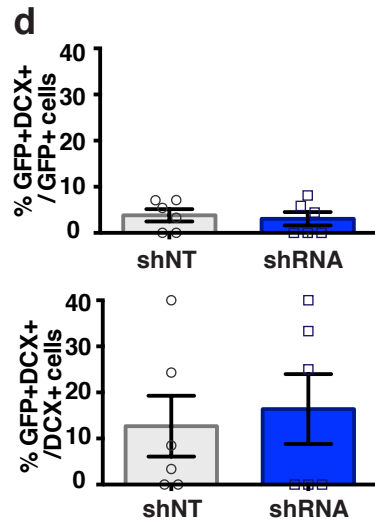
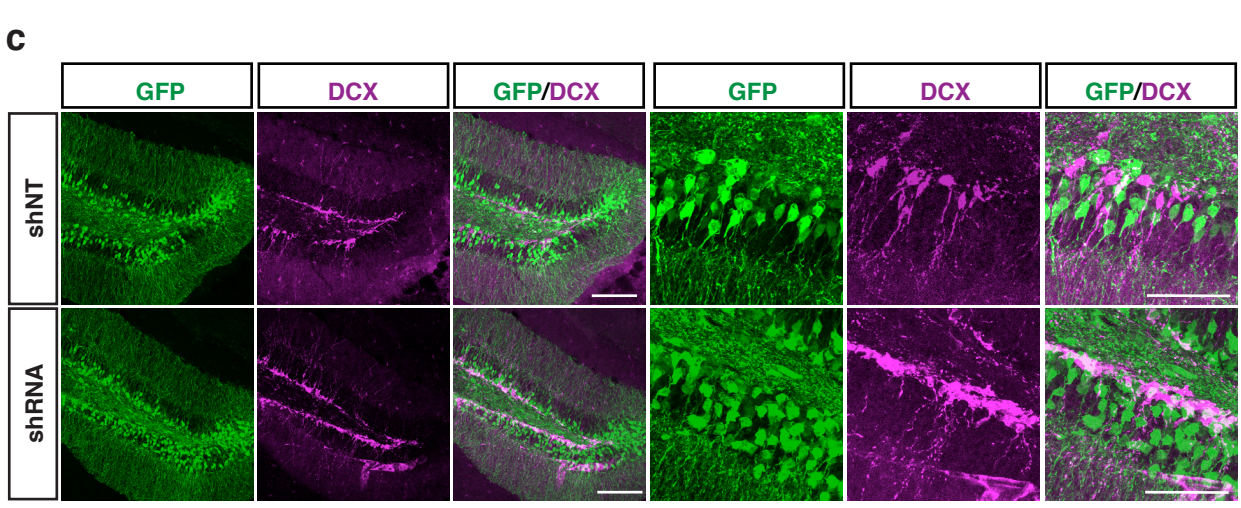
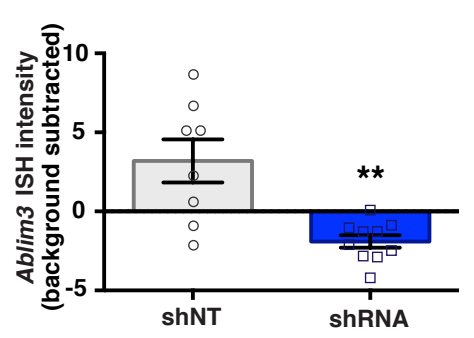
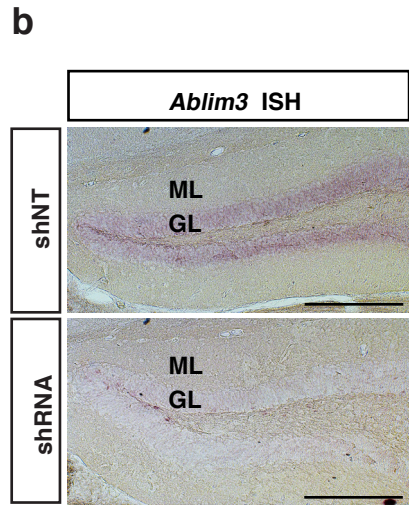
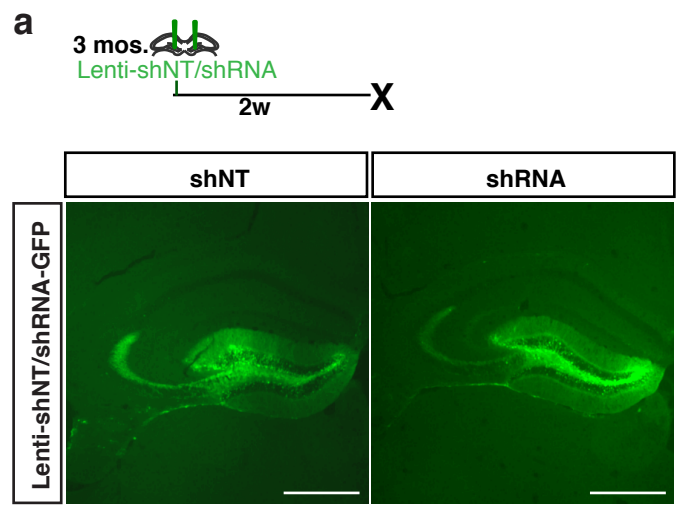
(a) Schematic of lentiviral-shNT/shRNA injections into DG (*upper*). Representative images show *in vivo* infection is restricted to DG (*lower*). Scale bar represents 500  $\mu$  m. This experiment was replicated more than 3 times.

(b) Representative *in situ* hybridization (ISH) images showing downregulation of *Ablim3* transcripts in DG following lentiviral-shNT/shRNA injections (*left*). Bargraph showing quantification of *Ablim3* expression in DG (raw pixel value) following background subtraction [Molecular layer (ML) in DG] (*right*, unpaired t-tests,  $p = 0.001$ ,  $n = 8, 9$  mice). Negative value in shRNA group is due to lower raw pixel value measured in Granule layer (GL) than Molecular layer (ML) in DG. Scale bar represents 100  $\mu$  m.

(c) Representative images showing overlap of Doublecortin (DCX+) immature adult-born DGCs and lentiviral-shNT/shRNA-GFP. Scale bar represents 100  $\mu$  m (*left 3 panels*) and 50  $\mu$  m (*right 3 panels*).

(d) Bar graphs showing quantification of images in C ( $n = 6, 6$ ).

\*\*\* $p < 0.001$ , \*\* $p < 0.01$ , \* $p < 0.05$ . Data are represented mean  $\pm$  SEM.



**Supplementary Figure 4. Supporting data for optogenetic activation of DG engram using Tet-Tag mice and following abLIM3 downregulation in DG.**

(a) Representative images of ChR2-eYFP expression in DG of cfos-tTA mice injected with AAV<sub>9</sub> tetO-channelrhodopsin (ChR2)-enhanced yellow fluorescent protein (eYFP), but not lentiviral shRNA/shNT RNA, at day 2 and day 10. Note, ChR2-eYFP distribution in DGCs illuminates the dendritic trees and cell bodies (arrows), whereas the green cell nuclei signal (arrowheads) is due to the 2-h half-life EGFP expression associated with the cfos-tTA line (see Methods). Box highlights magnified regions from each time point (*left*). Bar graphs showing quantification of ChR2-eYFP<sup>+</sup> cells with clear dendritic trees in DG at different time points. Scale bar, 200  $\mu$  m and 50  $\mu$  m.

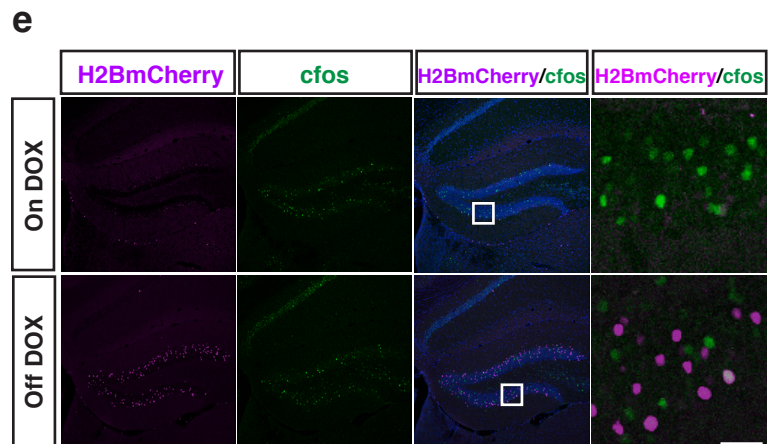
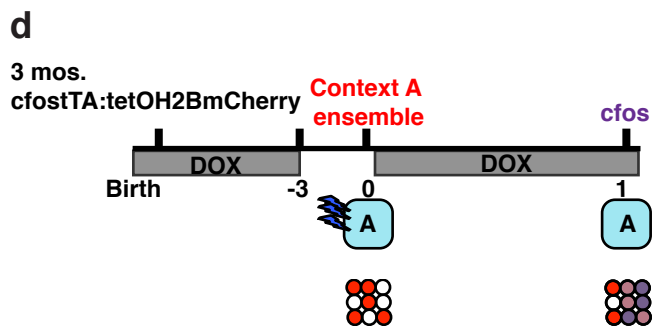
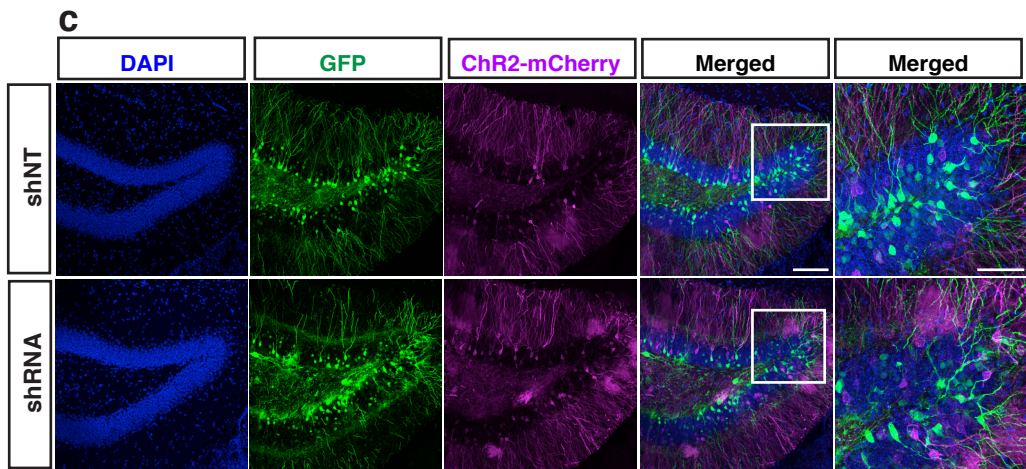
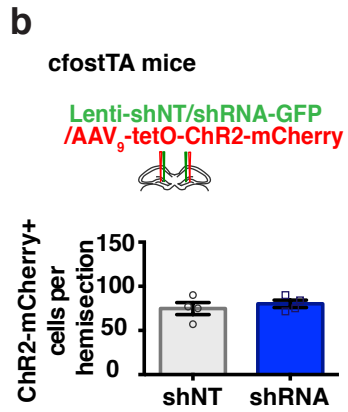
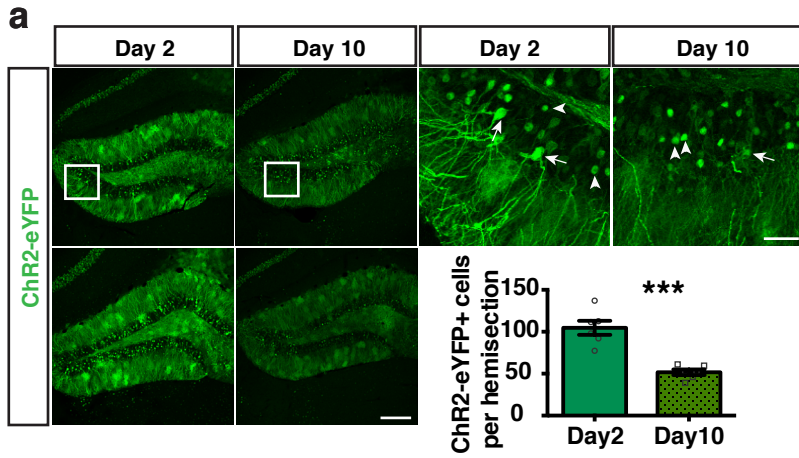
(b) Schematic of lentiviral shRNA/shNT-GFP and AAV<sub>9</sub> tetO-channelrhodopsin (ChR2)-mCherry injections into DG. Bar graphs showing quantification of ChR2-mCherry<sup>+</sup> cells in DG at day 10 (unpaired t-tests, n=4, 4 mice).

(c) Representative images showing lentiviral GFP and ChR2-mcherry expression in DG of cfos-tTA mice 10 days after injection of lentiviral shRNA/shNT-GFP and AAV<sub>9</sub> tetO-ChR2-mCherry. Box highlights magnified regions from each group (*right*). Scale bar, 100  $\mu$  m and 50  $\mu$  m.

(d) Schematic of cfos-tTA; H2BmCherry transgenic system to indelibly tag activity dependent neuronal ensembles during training and permit assessment of reactivation by cfos staining following context exposure.

(e) Representative images showing tight control of H2BmCherry expression in DG of cfos tTA:tetO H2BmCherry mice by DOX. Mice were conditioned to 3 footshocks in context A and perfused for cfos analysis following re-exposure to context A 24 hours later. Scale bar, 200  $\mu$  m and 50  $\mu$  m. This experiment was replicated with 4 mice per condition.

\*\*\*p < 0.001, \*\*p < 0.01, \*p < 0.05. Data are represented mean  $\pm$  SEM.



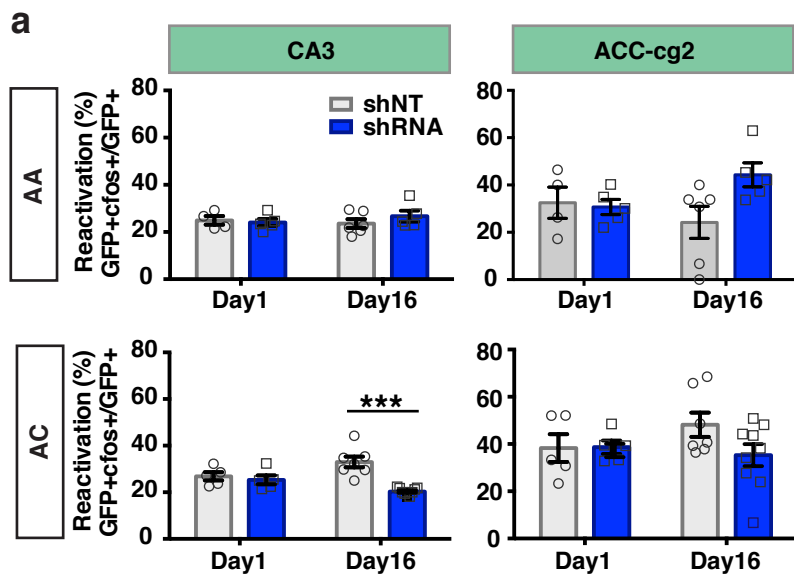
**Supplementary Figure 5. Supporting data for analysis of ensemble reactivation in hippocampal-cortical and BLA networks using Tet-Tag mice and following abLIM3 downregulation in DG.**

(a) Reactivation assessed by quantifying percentage of tagged H2BGFP+ cells in CA3 (left) and ACC-cg2 (right) that are cfos+ following re-exposure to context A and context C at day 1 and day 16 (Reactivation in AC group: CA3, Two-way ANOVA, day X treatment (shRNA vs. shNT virus),  $F(1, 22) = 11.09$ ,  $p = 0.003$ , Bonferroni post hoc,  $p < 0.0001$ ). AA-day1, n=4, 5 mice; AA-day16, n=6, 5 mice; AA-day1, n=5, 5 mice; AC-day16, n=7, 9 mice.

(b-d) Table (b) and bar graphs (c-d) summarizing the number of tagged H2BmCherry and H2BGFP cell counts. Both shNT and shRNA injected groups of mice had equivalent numbers of tagged cells in hippocampal-cortical and BLA networks. (DG-AA-day1, n=4, 4 mice; DG-AA-day16, n=5, 4 mice; DG-AC-day1, n=4, 4 mice; DG-AC-day16, n=6, 4 mice; CA3-AA-day1, n=4, 4 mice; CA3-AA-day16, n=5, 4 mice; CA3-AC-day1, n=4, 4 mice; CA3-AC-day16, n=6, 4 mice; CA1-AA-day1, n=4, 5 mice; CA1-AA-day16, n=5, 5 mice; CA1-AC-day1, n=5, 5 mice; CA1-AC-day16, n=6, 9 mice; ACC-cg1-AA-day1, n=4, 5 mice; ACC-cg1-AA-day16, n=6, 5 mice; ACC-cg1-AC-day1, n=5, 5 mice; ACC-cg1-AC-day16, n=7, 9 mice; ACC-cg2-AA-day1, n=4, 5 mice; ACC-cg2-AA-day16, n=6, 5 mice; ACC-cg2-AC-day1, n=5, 5 mice; ACC-cg2-AC-day16, n=7, 9 mice; BLA-AA-day1, n=4, 5 mice; BLA-AA-day16, n=6, 5 mice; BLA-AA-day1, n=5, 5 mice; BLA-AC-day16, n=7, 9 mice; CA3(tetOH2B)-AA-day1, n=4, 5 mice; CA3(tetOH2B)-AA-day16, n=6, 5 mice; CA3(tetOH2BGFP)-AA-day1, n=5, 5 mice; CA3(tetOH2B)-AC-day16, n=7, 9 mice). Two mice were excluded from CA1-AA-day16 shNT and CA1-AC-day16 shNT group analysis because there were no tagged cells detectable in CA1 pyramidal layer. Data are represented mean  $\pm$  SEM.

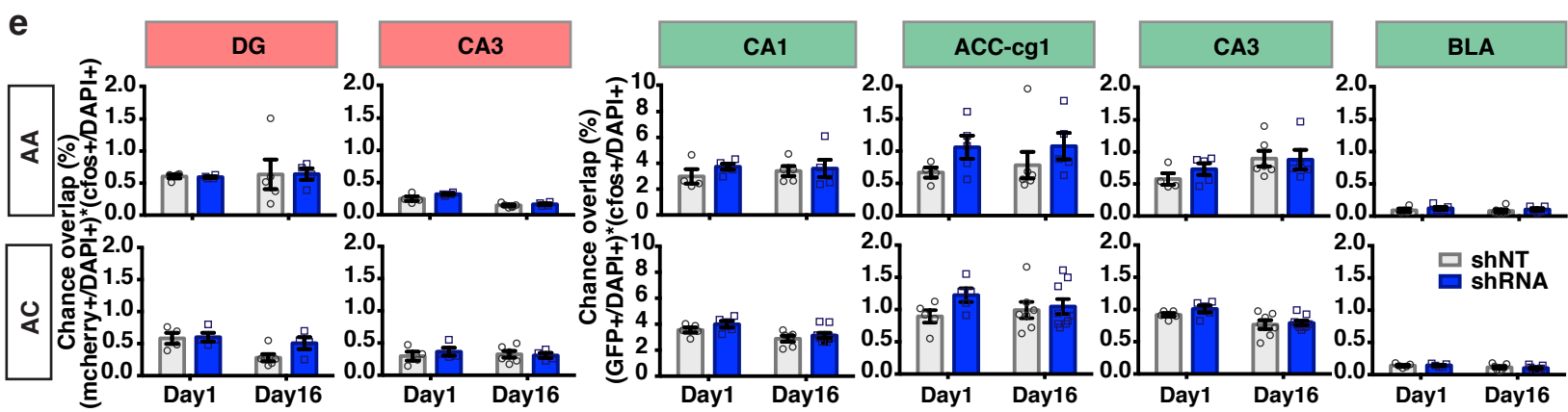
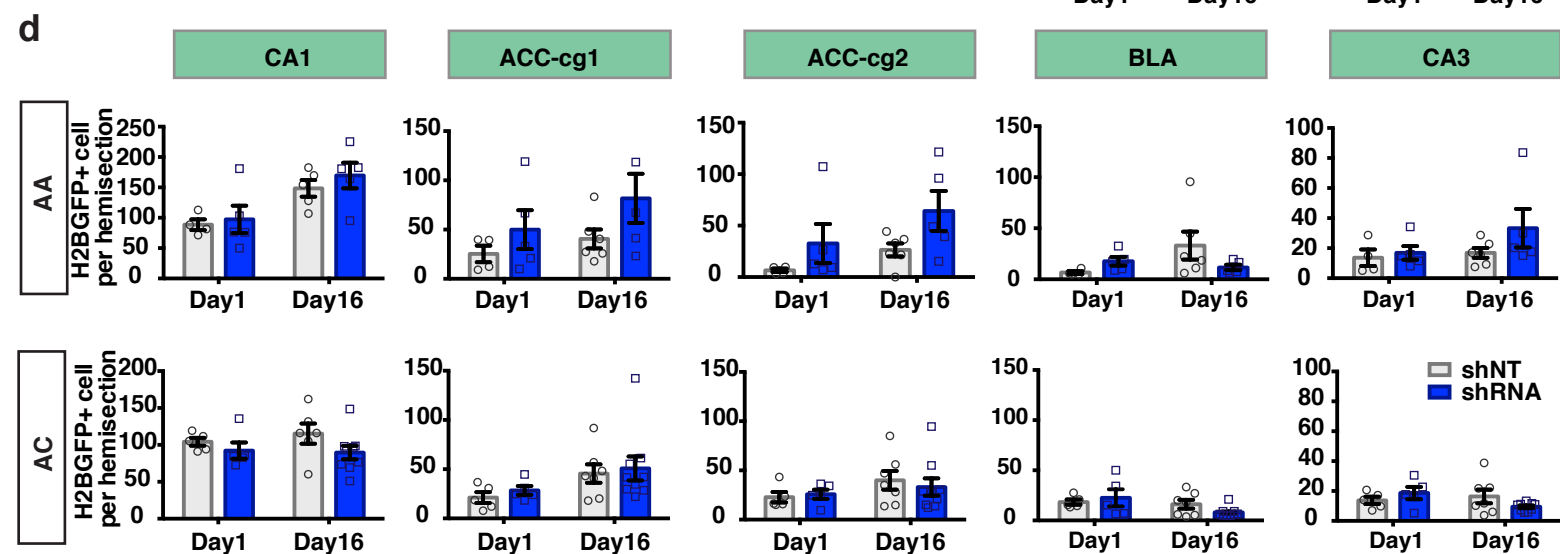
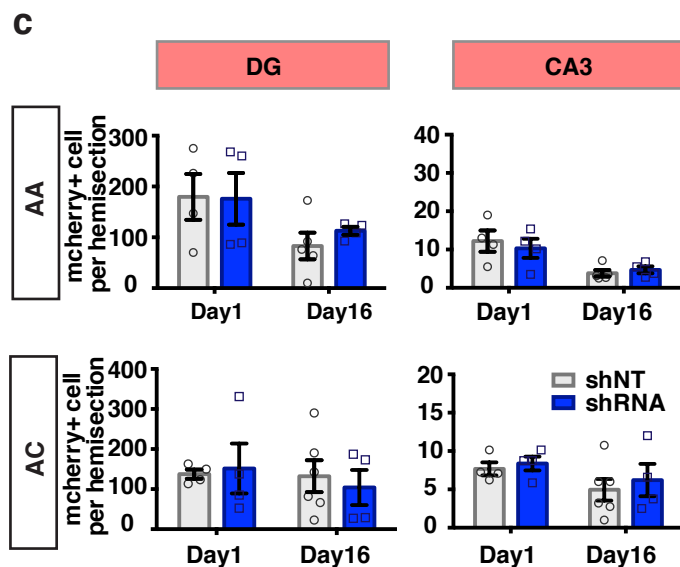
(e) Quantification of chance overlap of H2BGFP or H2BmCherry+ cells and cfos+ cells in DG, CA3 (cfostTA:tetOH2BmCherry transgenic), CA1, ACC-cg1, CA3 (cfostTA:tetOH2BGFP transgenic) and BLA at different time points. Both shNT and shRNA injected groups of mice exhibited comparable percentages of chance overlap in hippocampal-cortical and BLA networks.

\*\*\* $p < 0.001$ , \*\* $p < 0.01$ , \* $p < 0.05$ . Data are represented mean  $\pm$  SEM.

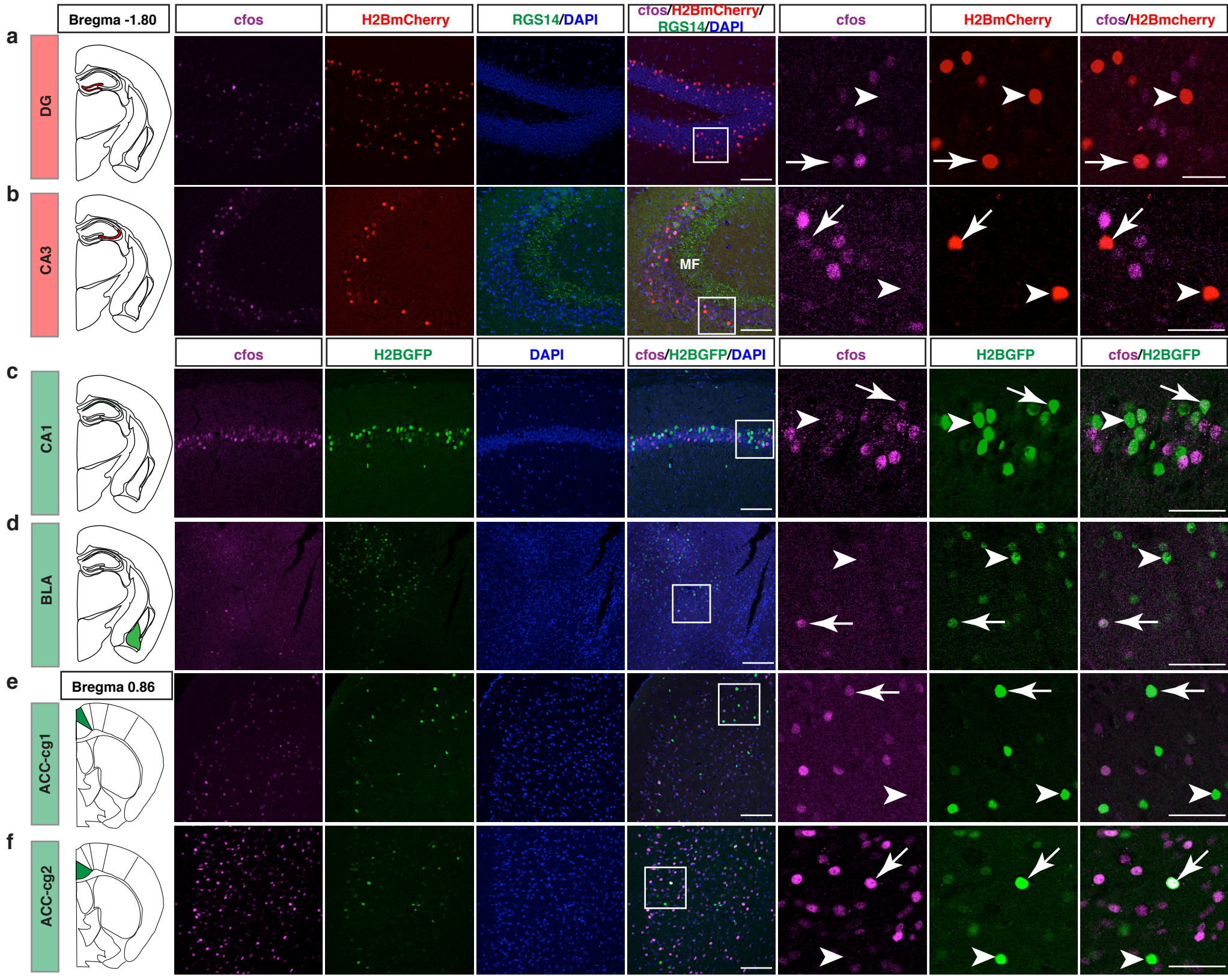


**b**

	AA				AC			
	Day 1		Day 16		Day 1		Day 16	
	shNT	shRNA	shNT	shRNA	shNT	shRNA	shNT	shRNA
DG	237	335	617	415	1263	773	1611	1750
CA3	141	213	250	130	256	376	138	169
CA1	1417	1947	2967	4061	2085	1845	2765	3227
ACC-cg1	604	659	1022	557	423	525	1295	1925
ACC-cg2	158	318	1018	792	455	491	1160	1089
CA3	327	506	606	999	412	558	688	505
BLA	106	353	792	232	366	452	453	289



**Supplementary Figure 6. Representative images showing tagged ensembles in Tet-Tag mice using H2B mCherry and H2B GFP alleles.** H2BmCherry tagged neurons in DG (a) and CA3 (b), H2BGFP tagged neurons in CA1 (c), BLA (d), ACC-Cg1 (e) and ACC-Cg2 (f) expressing *cfos*<sup>+</sup> (arrows) or devoid of *cfos* expression (arrowheads). RGS14 staining (Green in b) in pyramidal cell layer was used to exclude CA2 cells counts. GFP<sup>+</sup> mossy fiber (MF in b) track was from lentiviral GFP infection of granule neurons in DG. White boxes indicate regions magnified in the 3 right panels. Scale bar represents 100  $\mu$  m (*left 4 panels*) and 50  $\mu$  m (*3 right panels*). The immunostaining was replicated in all tet-tag cohorts of mice shown in Figure 4d-g and supplementary figure 5a-5e.



**Supplementary Figure 7. Downregulation of abLIM3 in DG does not affect DG activity when mice are exposed to neutral, distinct context at remote timepoint and also does not affect innate anxiety and behavioral despair in adult mice.**

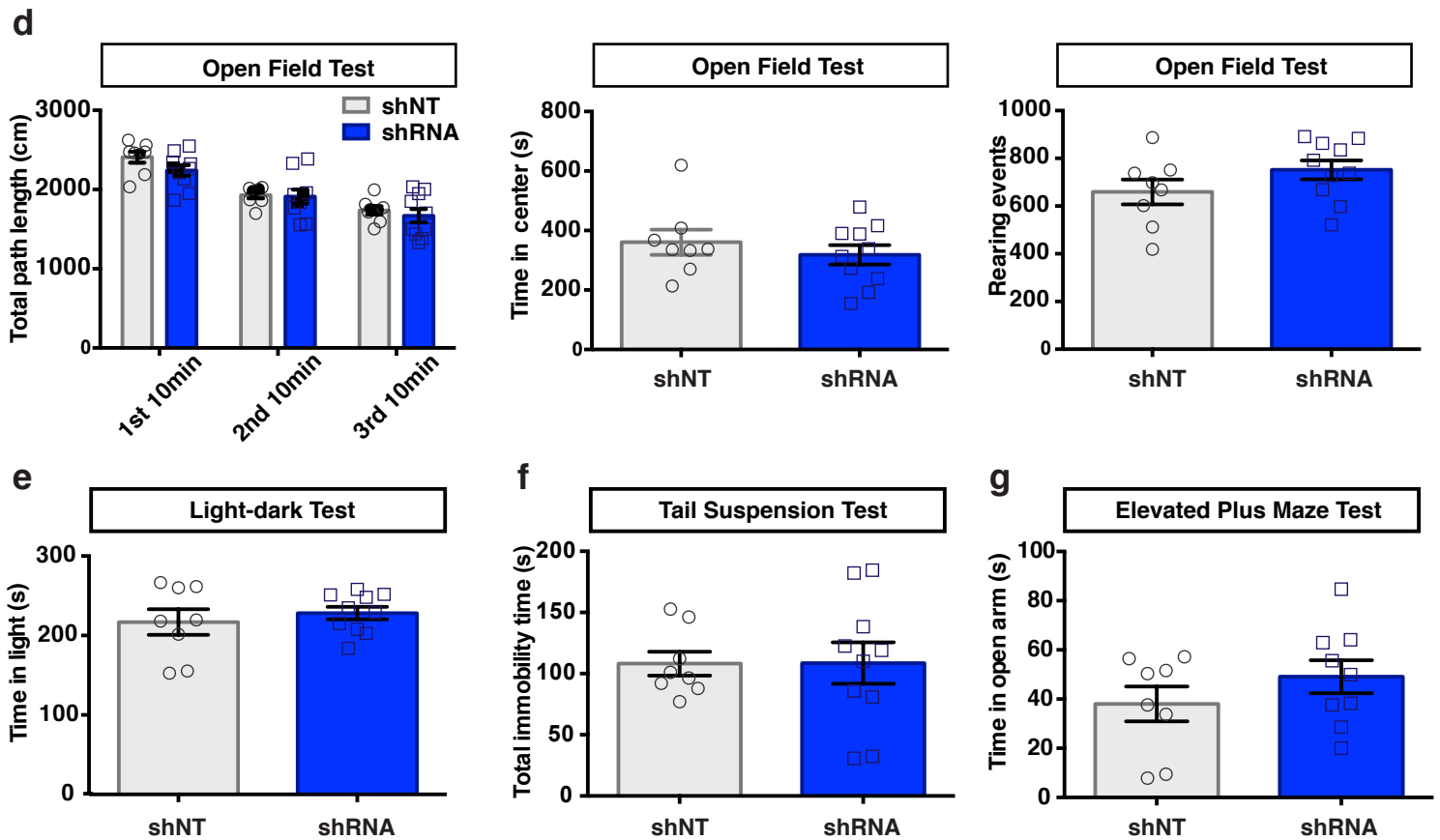
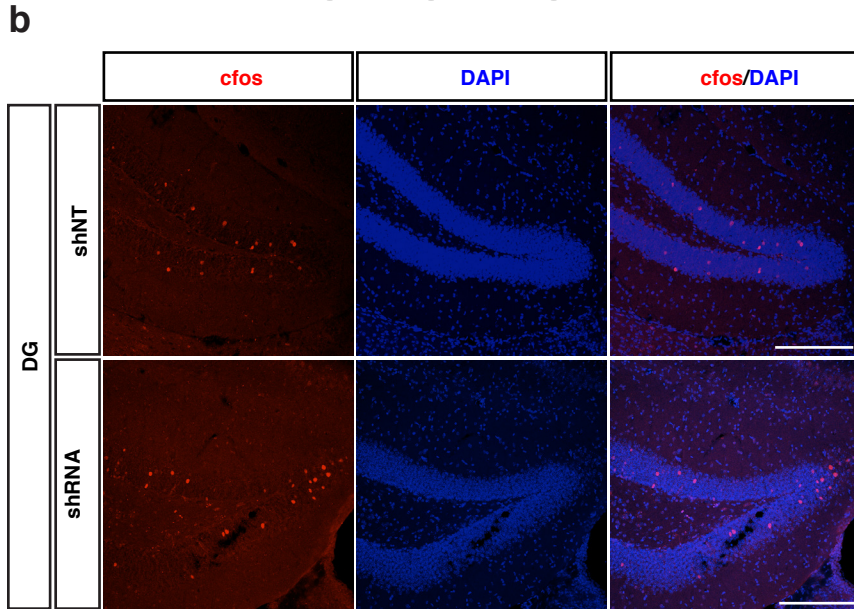
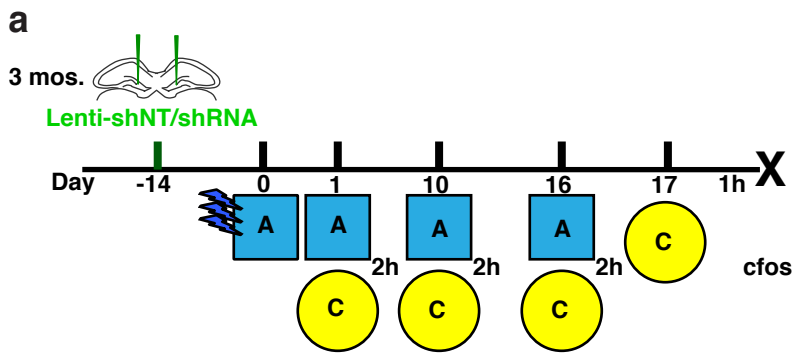
(a) Schematic of Lentiviral-shNT/shRNA injection into DG and contextual fear conditioning paradigm with intervening exposures.

(b) Representative images showing *cfos*<sup>+</sup> population in DG after context C exposure at day 17 (*left*). Bar graph showing quantification of *cfos*<sup>+</sup> cell counts (*right*) (n=8, 10 mice). Scale bar represents 100  $\mu$  m.

(c) Schematic of behavioral paradigm of lentiviral-shNT/shRNA injected 3-month old mice to probe for changes in locomotor activity, innate anxiety and antidepressant-like behavioral effects. abLIM3 downregulation in DG does not affect locomotor activity, innate anxiety or antidepressant-like behavioral effects.

(d) Open field test (n=8, 10 mice) (e) light-dark test (n=8, 10 mice), (f) tail suspension test (n=8, 10 mice) and (g) elevated plus maze test (n=8, 9 mice, one mouse from shRNA group jumped out of EPM and was excluded from EPM analysis).

\*\*\*p < 0.001, \*\*p < 0.01, \*p < 0.05. Data are represented mean  $\pm$  SEM.



**Supplementary Figure 8. Downregulation of abLIM3 in DG increases activation of PV-INs but not SST-INs in CA3 after context A exposure at remote time point in adult mice.**

(a) Schematic of lentiviral shNT/shRNA injections and behavioral testing schedule.

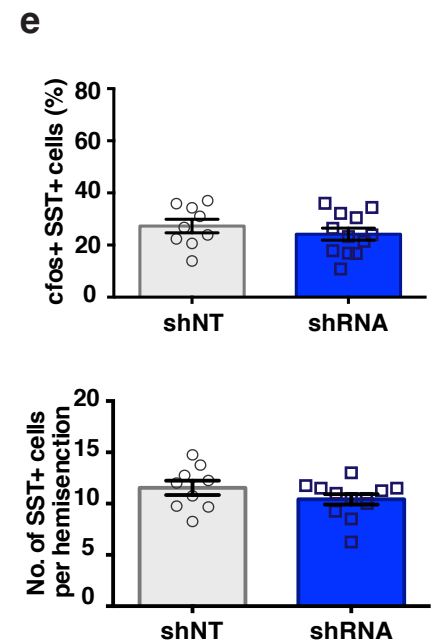
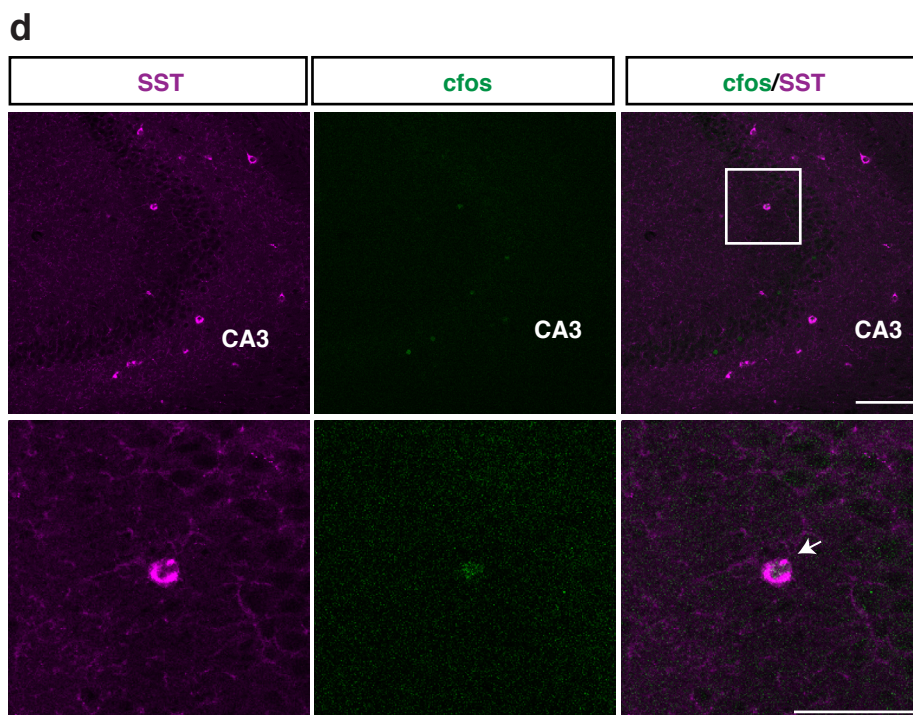
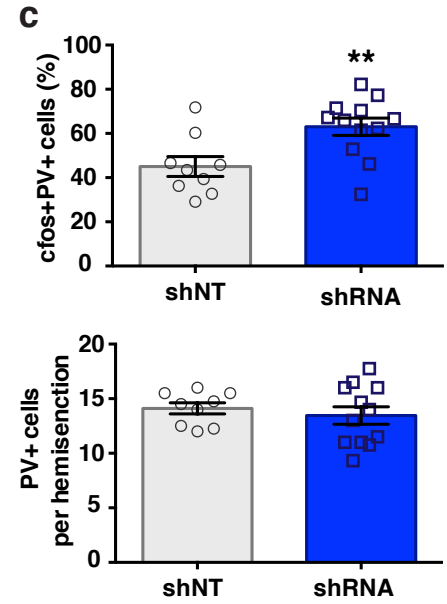
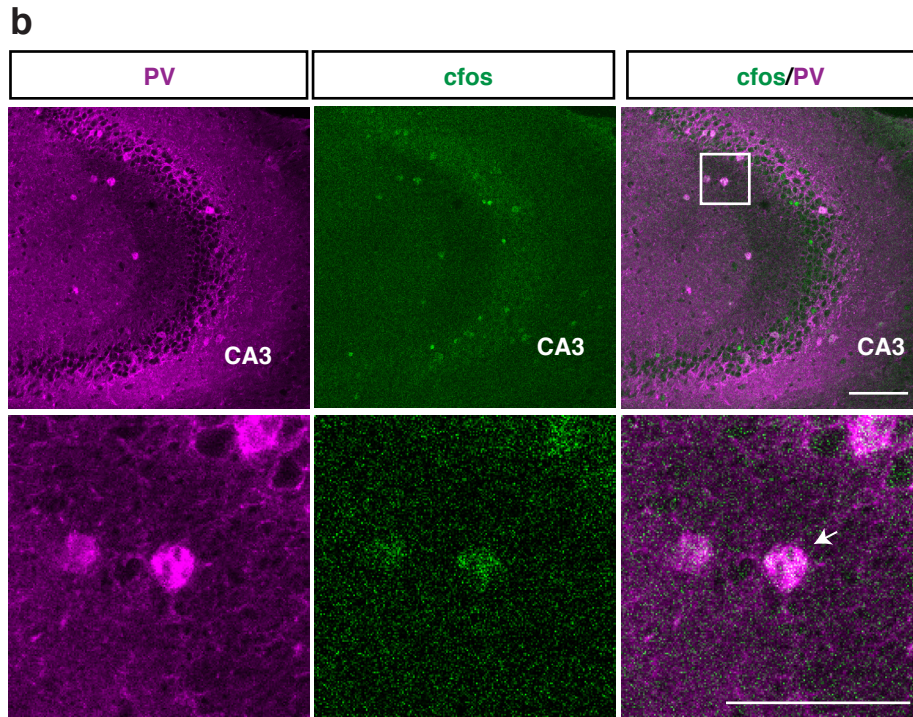
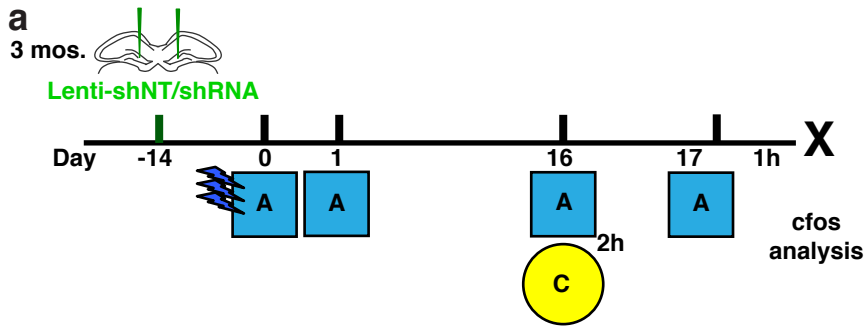
(b) Confocal images show cfos+PV+ cells (arrow) in CA3 area after context A exposure at day 17. Scale bar represents 100  $\mu$  m and 50  $\mu$  m .

(c) Bar graph with quantification of percentage of cfos+PV+ cells over total PV+ cells (*upper*) and total PV+ cells counts in CA3 area (unpaired t-tests , n=9,12 mice).

(d) Confocal images show cfos+SST+ cells (arrow) in CA3 area after context A exposure at day 17. Scale bar represents 100  $\mu$  m and 50  $\mu$  m .

(e) Bar graph with quantification of percentage of cfos+SST+ cells over total SST+ cells (*upper*) and total SST+ cells counts in CA3 area (unpaired t-tests , n=9,12 mice).

\*\*\*p < 0.001, \*\*p < 0.01, \*p < 0.05. Data are represented mean  $\pm$  SEM.



**Supplementary Figure 9. Supporting data for analysis of abLIM3 downregulation in DG of aged mice.**

(a) Schematic of lentiviral shNT/shRNA injections (*left*), image based renderings from Fig.6c (*bottom left*) and bar graphs (*right*) conveying MFT filopodia number (Fig. 6c), MFT filopodia length and MFT size following lentiviral-shNT/shRNA injection into DG of 17-month old mice (unpaired t-tests, MFT size,  $P = 0.6678$ ; filopodia length,  $p = 0.003$ ,  $n=3, 4$  mice).

(b) Representative images showing GFP+ DGC dendrites in outer molecular layer (OML) following lentiviral-shNT/shRNA injection into DG of 17-month old mice (*left*). Bar graph showing quantification of DGC spine density (*right*, unpaired t-tests,  $P=0.9013$ ,  $n=3$  mice for each group). Scale bar represents  $10 \mu\text{m}$ .

(c) Representative image (*left*) and quantification (*right*) showing percentage of GFP+VGLUT1+ MFT-filopodia contacting PV SLINs ( $n=3,4$  mice) following lentiviral-shNT/shRNA injection into DG of 17 months old mice. Scale bar represents  $5 \mu\text{m}$ .

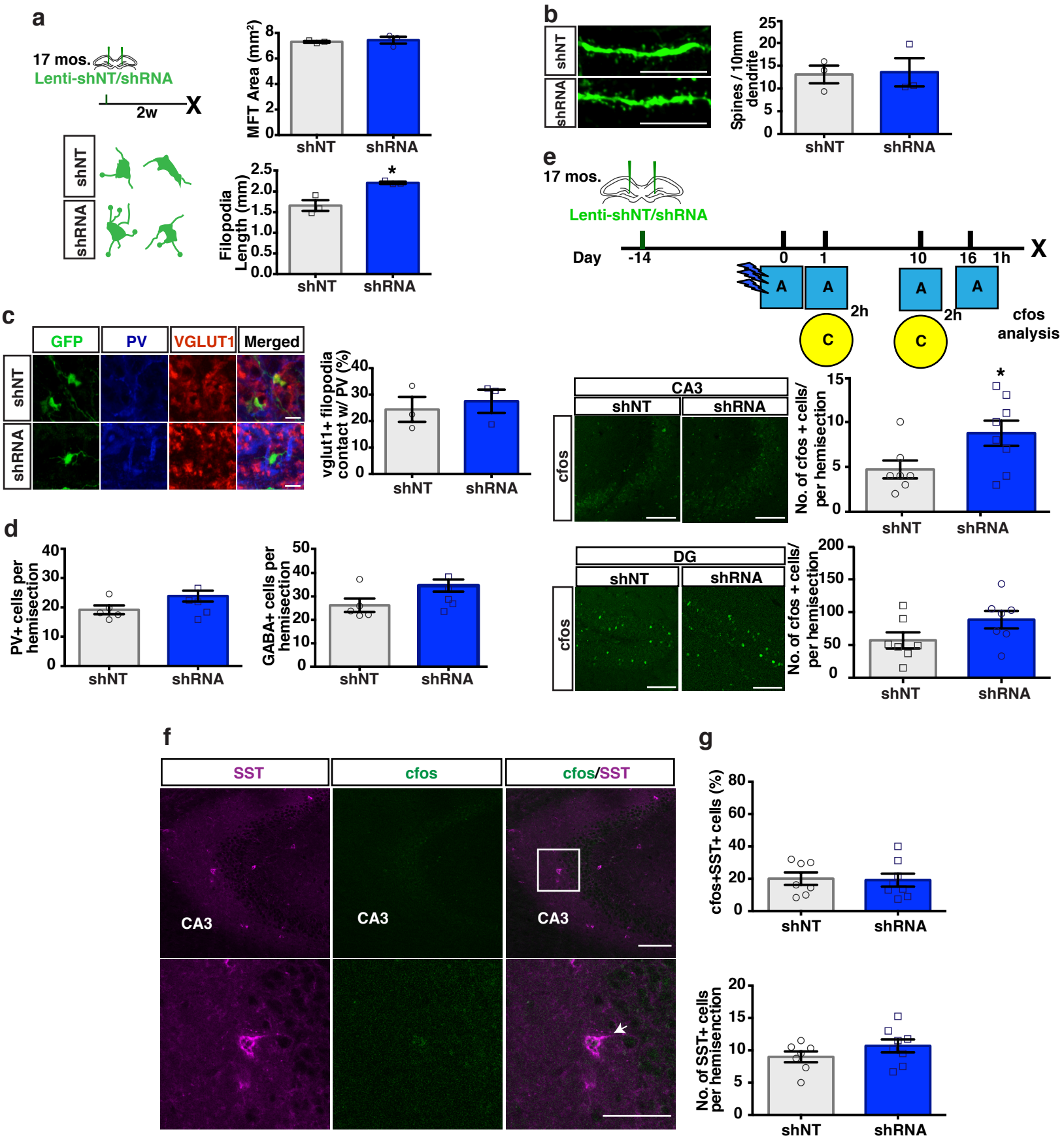
(d) Quantification of total number of PV and GABA+ cells in count in CA3 of 17 months old mice (corresponds to Fig. 6e,  $n=5,5$  mice).

(e) Schematic of contextual fear conditioning paradigm with multiple contextual exposures used to test 17-month old mice (*upper*). Representative images and bar graphs showing quantification of cfos+ population in CA3 pyramidal layer (*middle*, unpaired t-tests,  $P=0.0406$ ,  $n=7, 8$  mice for each group) and DG granule layer (*lower*, unpaired t-tests,  $P=0.1054$ ,  $n=7, 8$  mice for each group). Scale bar represents  $100 \mu\text{m}$ .

(f) Confocal images showing cfos+SST+ cells (arrow) in CA3 after context A exposure at day 16. Scale bar represents  $100 \mu\text{m}$  and  $50 \mu\text{m}$ .

(g) Bar graph with quantification of percentage of cfos+SST+ cells over total SST+ cells (*upper*) and total SST+ cells counts in CA3 area after context A exposure at day 16 (unpaired t-tests,  $n=7,8$  mice).

\*\*\* $p < 0.001$ , \*\* $p < 0.01$ , \* $p < 0.05$ . Data are represented mean  $\pm$  SEM.

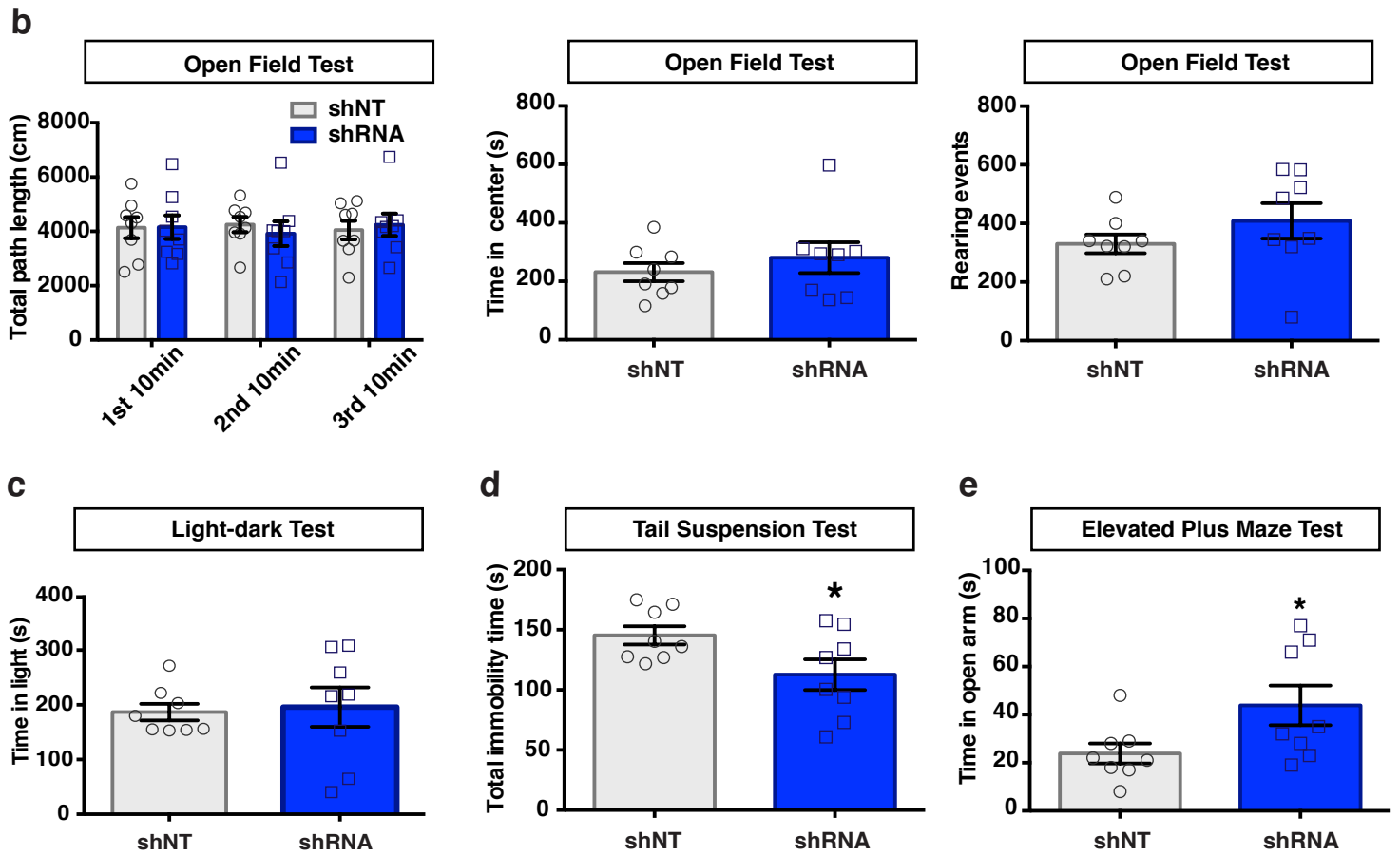
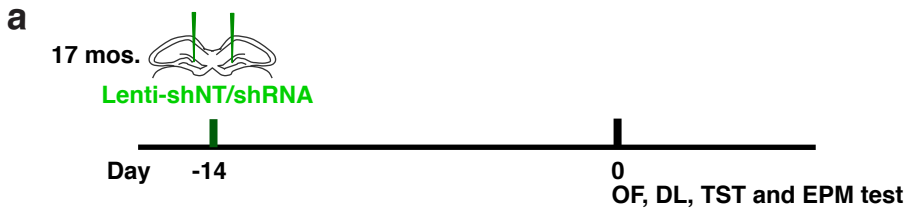


**Supplementary Figure 10. Analysis of innate anxiety and behavioral despair in aged mice**

(a) Schematic of behavioral paradigm of lentiviral-shNT/shRNA injected 17-month old mice to probe for changes in locomotor activity, innate anxiety and antidepressant-like behavioral effects.

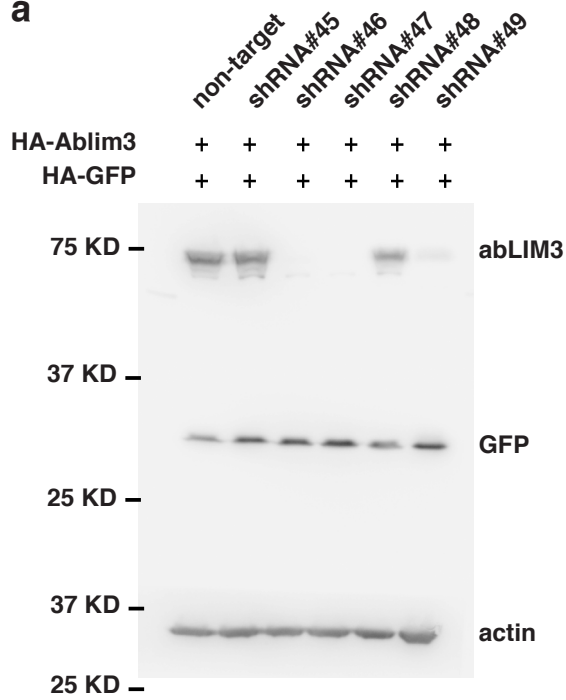
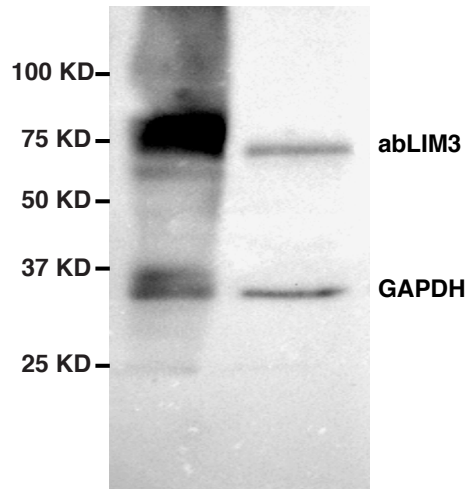
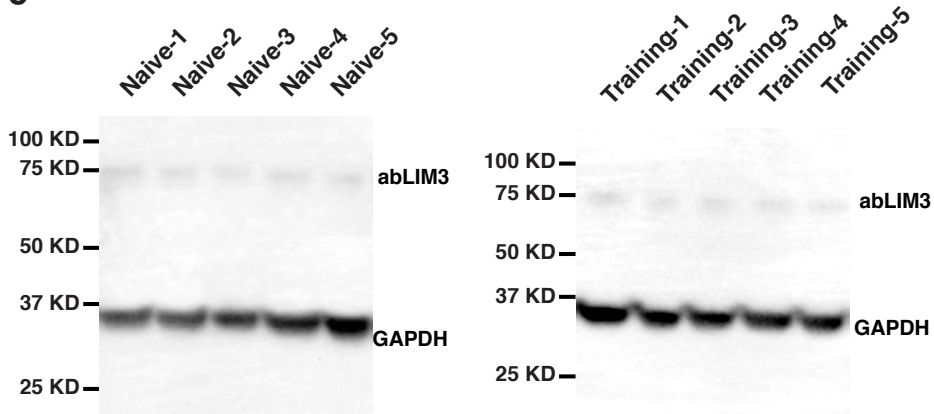
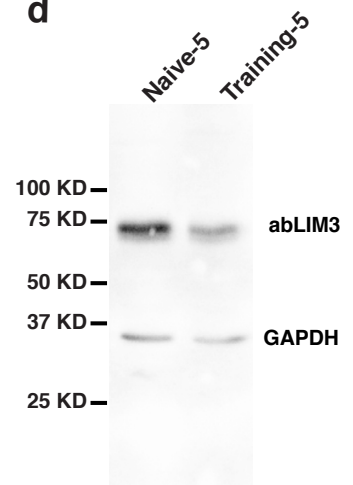
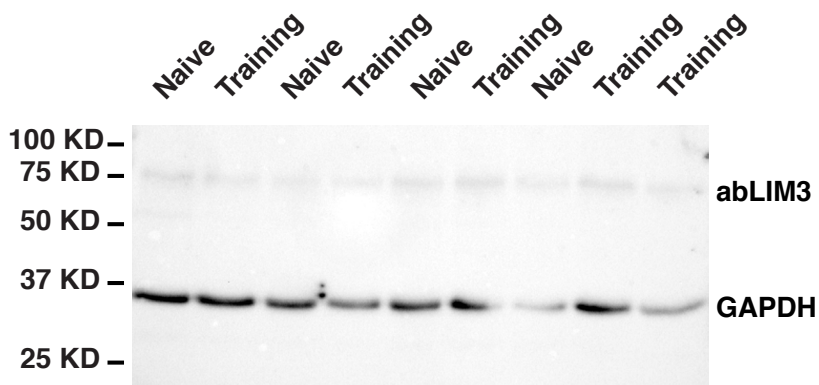
(b) Open field test (n=8, 8 mice), (c) Light-Dark test (n=8, 8 mice), (d) tail suspension test (n=8, 8 mice) and (e) elevated plus maze test (n=8, 8 mice).

\*\*\*p < 0.001, \*\*p < 0.01, \*p < 0.05. Data are represented mean ± SEM.



### **Supplementary Figure 11. Full scans of western blots**

- (a) Full scan of western blot showing shRNA mediated knockdown of abLIM3 in 293K cells (corresponding to supplementary Fig. 2a).
- (b) Full scan of western blot showing validation of abLIM3 antibody (corresponding to supplementary Fig. 1c).
- (c) Full scan of western blot showing abLIM3 levels in hippocampus at baseline and after learning (n=5 mice per group). These blots were used for quantification shown in bar graphs in Fig. 1e (mouse GAPDH 1:2000, rabbit abLIM3 1:500, rabbit HRP: 1:5000, mouse HRP: 1:5000).
- (d) Full scan of western blot showing abLIM3 levels in hippocampus at baseline and after learning from a single mouse corresponding to blot shown in Fig. 1e (mouse GAPDH 1:4000, rabbit abLIM3 1:500, rabbit HRP: 1:5000, mouse HRP: 1:10,000).
- (e) Full scan of western blot showing abLIM3 levels in CA1 at baseline and after learning (corresponding to supplementary Fig. 1d). n=4,5 mice per group (mouse GAPDH 1:2000, rabbit abLIM3 1:500, rabbit HRP: 1:5000, mouse HRP: 1:5000).

**a****b****c****d****e**

**Supplementary Figure 12. Model conveying how DGC recruitment of feedforward inhibition onto CA3 dictates memory engram maintenance, constrains reactivation of remote memory traces in CA3-ACC-BLA networks and decreases remote memory generalization.**

(a) *For a limited time period*, a context associated with a footshock (context A) is encoded and stored in blue neurons in DG-CA3 circuit. Within CA3, the context A ensemble is made up of highly specific (dark blue) and less specific (light blue) context A neurons. *Over time and for long as the engram persists in the DG*, the corresponding representation of context A is consolidated in blue neurons in the ACC and BLA, presumably during sharp-wave ripples and through mechanisms such as replay (indicated by black arrows in a loop). As in CA3, the context A ensemble in ACC and BLA is made up of highly specific (dark blue) and less specific (light blue) context A neurons. At a remote time point, exposure to a neutral, distinct context C activates yellow neurons in DG-CA3 circuit. *Because the DG engram becomes silent over time and no longer recruits sufficient inhibition onto CA3*, some light blue context A neurons in CA3 are also reactivated (shown as green neurons) which results in reactivation of entire context A trace in CA3-ACC-BLA networks. The reactivation of context A memory traces in CA3-ACC-BLA by exposure to context C elicits freezing behavior in context C.

(b) Increasing DGC recruitment of inhibition onto CA3 *ensures that the context A trace in CA3 is made up of mostly dark blue neurons and few light blue neurons*. Additionally and importantly, *it maintains the context A memory engram in DG at remote timepoints*. *The maintenance of the engram in the DG promotes CA3-ACC-BLA communication* presumably via mechanisms such as replay (indicated by black arrows in a loop) *resulting in enhanced consolidation of the context A ensemble in ACC and BLA*. *Because of sustained engram bearing DGC recruitment of inhibition onto CA3*, exposure to a neutral, distinct context C at remote time points activates yellow neurons in DG-CA3 circuit and very few light blue CA3 context A neurons. This, in turn, constrains reactivation of context A blue neurons in ACC and BLA, and consequently, decreases levels of freezing in context C. Dashed lines indicate ACC dependent and independent pathways by which the DG engram may govern consolidation of memory traces in BLA.

